Effect of transformed β phase on fish-eye ductile crack initiation of a Ti-6Al-4V alloy in very high cycle fatigue regime

Tao Gao, Hongqian Xue, Zhidan Sun

Effect of transformed β phase on fish-eye ductile crack initiation of a Ti-6Al-4V alloy in very high cycle fatigue regime

Tao Gao[1], Hongqian Xue[1*], Zhidan Sun[2*]

[1]School of mechanical engineering, Northwestern Polytechnical University, Xi'an 710072 China

[2] ICD, P2MN, LASMIS, University of technology of Troyes, CNRS FRE2019, Troyes, France

Corresponding author[1*]: xuedang@nwpu.edu.cn, +86 15991715727

Corresponding author[2*]: zhidan.sun@utt.fr, +33 3 25 71 80 62

Abstract

Very high cycle fatigue (VHCF) properties and damage mechanisms were investigated for a Ti-6Al-4V alloy with needle-like β phase. It was revealed that the fatigue damage is dominated by interior crack initiation with a fish-eye pattern. The center of the fish-eye area is covered by peaks, dimples, microvoids and grooves, exhibiting micro-ductile characteristics instead of the commonly reported brittle ones. It was found that the formation of this particulier appearance resulted from the nucleation and coalescence of microvoids and grooves essentially occurring in the transformed β phase (β_t). The β_t phase played a dominant role in the crack initiation process of the Ti-6Al-4V in the VHCF regime.

Keywords: Titanium alloy; Microstructure; Fatigue; Crack initiation; Ductile fracture

1. Introduction

Aero-engine components manufactured from titanium alloys such as compressor and turbine blades, are commonly subjected to fatigue loading of more than 1×10^7 cycles [1]. Therefore, very high cycle fatigue (VHCF) failure is one of the vital issues in aviation applications of titanium alloys. In the VHCF regime, crack initiation plays a determining role in fatigue properties, because it consumes more than 90% of the total fatigue life [2]. Compared to high cycle fatigue, VHCF usually results in special crack initiation morphologies at the interior of titanium alloys. A typical

example of these characteristics is the fish-eye pattern with a circular "bright rough area (BRA)" at its center [3]. BRA also named "Fine Granular Area (FGA)", "Granular Bright Facet (GBF)" and "Optically Dark Area (ODA)" in other references [3-5], is recognized as the interior crack initiation region. Understanding the mechanisms of the interior crack initiation is a top priority for the development and the application of titanium alloys subjected to VHCF.

As reported in the literature [5, 6], the BRA in titanium alloys is commonly covered by primary α (α_p) grain facets, characteristic of brittle fracture. These facets result from fractured α_p grains induced by slip activities under cyclic loading [7-10]. Recent studies revealed however, that β_t has a significant effect on slip activities [11, 12], such as slip transfer across α/β interface, which could influence the fatigue crack initiation process. Therefore, the β_t has a potential effect on the formation of the interior crack initiation area for α+β titanium alloys subjected to VHCF.

In this work, the VHCF properties of a Ti-6Al-4V alloy with needle-like β phase were investigated. A ductile fatigue damage feature of the α+β titanium alloy in the VHCF regime was highlighted. Damage mechanisms were analyzed and particular attention was given to the role played by the β_t in the formation of the interior crack initiation area.

2. Material and methods

A Ti-6Al-4V alloy with a chemical composition of Ti-6.45Al-4.1V-0.05Fe-0.16O-0.01N was investigated in this work. The alloy underwent an annealing treatment at a temperature of 740 ºC for 2h, followed by air cooling in a mill-annealed condition. Hourglass-shaped specimens with a minimum diameter of 4 mm were used in the fatigue testing experiment. Prior to fatigue testing, all the specimens were ground using SiC papers and subsequently electropolished. The fatigue tests were performed under symmetric tension-compression at room temperature using an ultrasonic fatigue testing system. The microstructure, fracture surface and the outer circumferential surface damage morphology of failed specimens were examined using a field emission gun scanning electron microscope (FEG-SEM).

3. Results and discussion

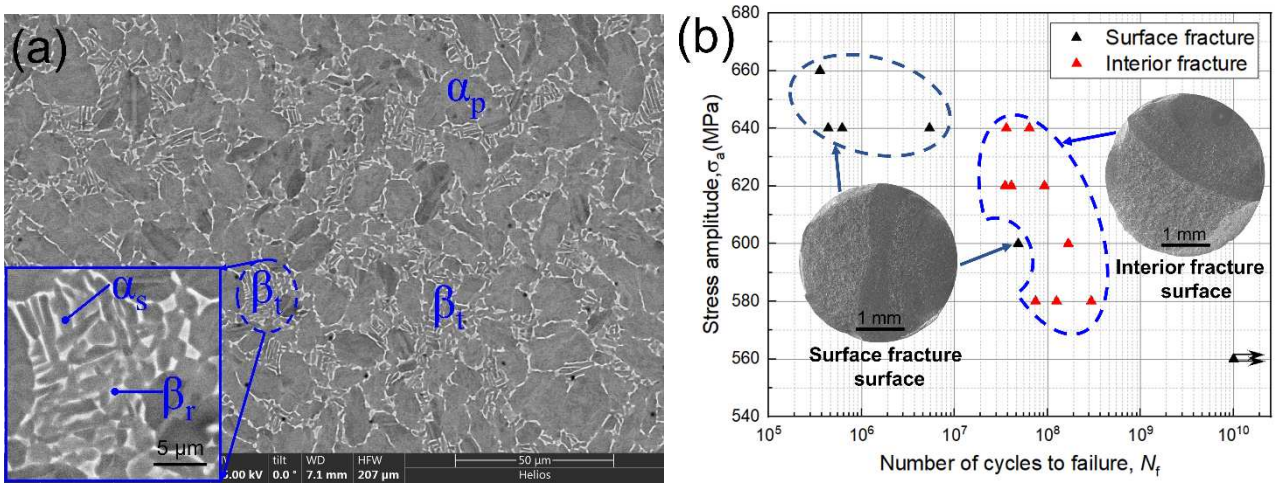

Fig. 1. (a) Backscattered micrograph of the investigated Ti-6Al-4V alloy and (b) *S-N* plot of the ultrasonic fatigue testing results for the studied Ti-6Al-4V alloy.

The microstructure illustrated in Fig. 1a has a bimodal morphology, composed of equiaxed primary α phase (α_p) and transformed β phase (β_t). β_t consists of secondary α phase (α_s) and retained β phase (β_r), as shown in the magnified image in Fig. 1a. The majority of α_s and β_r have a needle-like shape with a width of 0.5-1 μm and 0.1-0.35 μm, respectively. Few α_s and β_r exhibit near-globular shape. Image analysis revealed that the volume fraction of α phase is about 85%.

The applied stress amplitude (σ_a) versus the number of cycles to failure (N_f) plot is presented in Fig. 1b. It can be seen that the fatigue lives vary from about 3.56×10^5 cycles to 2.95×10^8 cycles for the applied stress levels ranging from 660 to 580 MPa. In the VHCF regime with fatigue life beyond 10^7 cycles, SEM micrographs reveal that crack initiation occurred at the interior for the majority of specimens. It can thus be concluded that the interior crack-induced failure is the primary damage mode for the studied Ti-6Al-4V alloy under VHCF loading.

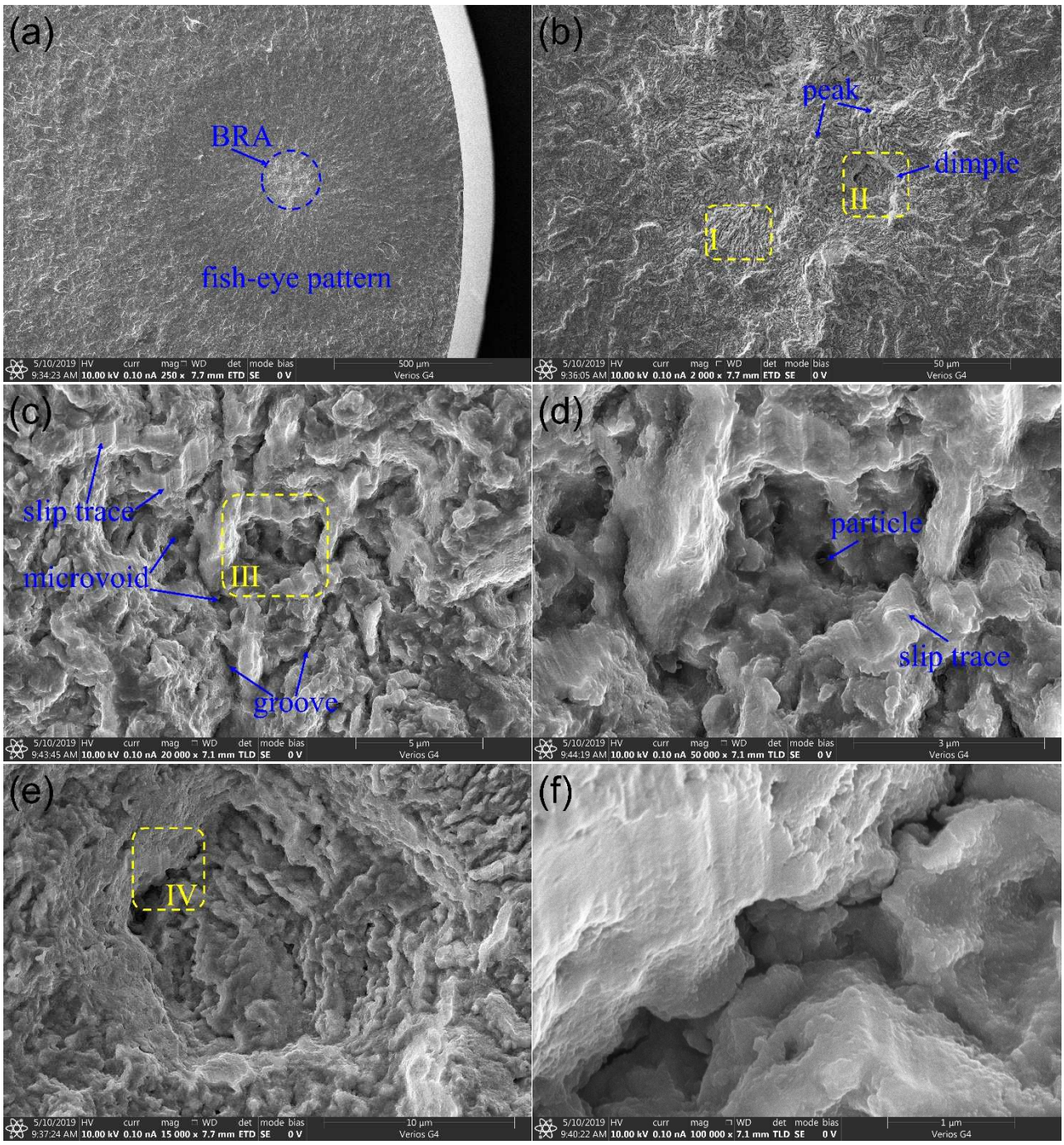

Fig. 2. Example of an interior-induced fracture surface (σ_a = 580 MPa, N_f = 1.25×10^8): (a) overall view of fish-pattern; (b) magnified image of the bright rough area (BRA) at the center of the fish-eye pattern; (c) magnified view of Area I in (b); (d) magnified view of microvoids in Area III in (c); (e) magnified view of a dimple in Area II in (b); (f) magnified view of grooves at the dimple bottom IV in (e).

Fig. 2 shows an example of representative fracture surface morphology obtained in the VHCF regime. A circular area with fish-eye pattern can be observed at the fracture surface. This is a typical characteristic of interior crack initiation and propagation in vacuum for α+β titanium alloys under VHCF. The bright rough area (BRA) at the center of the fish-eye pattern is the crack

initiation site, as shown in Fig. 2a and b. It was commonly reported in the literature that the BRA is characterized by facets resulting from α_p grains fractured in a transcrystalline manner in $\alpha+\beta$ titanium alloys [7-10, 13]. However, in our present work, no obvious facets or cleavage features can be observed in the BRA for the studied Ti-6Al-4V. In fact, this area is mainly characterized by rough dimples and peaks, as shown in Fig. 2b. The surface of peaks and small dimples are covered by rod-like particles, grooves and microvoids, as shown in Fig. 2c and d. Several nanoscale exfoliated particles can be observed at the bottom of grooves and microvoids. Moreover, slip traces are present in some surfaces of dimples. As for the large dimples, the bottom is separated by deep grooves and also covered by rod-like particles, as presented in Fig. 2e and f. These microscopic fractographic features indicate that the interior crack initiation is closely related to the nucleation and coalescence of microvoids and grooves, and the dominant microscopic mechanism of fracture is a ductile crack nucleation instead of brittle one.

Even though the specimen failed from the interior, some micro-damage characteristics should exhibit at the surface. Thus, outer circumferential surface morphologies near the fracture surface were also observed using SEM. An example of surface morphologies below interior crack-induced fracture surface is presented in Fig. 3. Slip traces, microcracks and microvoids can be observed on the specimen surface, as shown in Fig. 3a. Clear slip traces as well as some straight microcracks along the slip bands are located in α_p phase (Fig. 3b), while some microvoids are observed in β_t phase (Fig. 3c and d). Slip bands induced cracking in α_p would result in transgranular fracture and formation of facets on the fracture surface. However, as shown above, the interior crack initiation is characterized by micro-ductile damage with dimples and microvoids rather than transgranular facets. It can thus be deduced that the interior crack initiation is caused by the nucleation and coalescence of micro-voids in β_t phase. In contrast to the α_p phase or grains induced fracture commonly reported for titanium alloys under VHCF, the β_t phase plays a determining role in interior crack initiation of the studied Ti-6Al-4V alloy. These distinctive micro-ductile features of the BRA are ascribed to β_t morphology and distribution, as the retained β phase (β_r) has an obvious effect on micro-plastic deformation, such as slip transfer.

In titanium alloys, the β phase is harder than the α phase with a same microscale and thus has higher resistance to slip. The slip activity originating in α phase is the primary micro-deformation response of external cyclic loading in α+β titanium alloys [14, 15]. The motion of slip or dislocation originating from a soft α_s phase is blocked by adjacent β_r with a high misorientation [16], which gives rise to internal stress at α_s/β_r interfaces in the matrix. As the VHCF test continues, the internal stress concentration is gradually increased, and finally impels microcrack nucleation at α_s/β_r interfaces to accommodate the deformation mismatch in β_t. These microvoids in β_t coalesce to form the BRA and then the main crack propagates in vacuum, which gives birth to a fish-eye pattern.

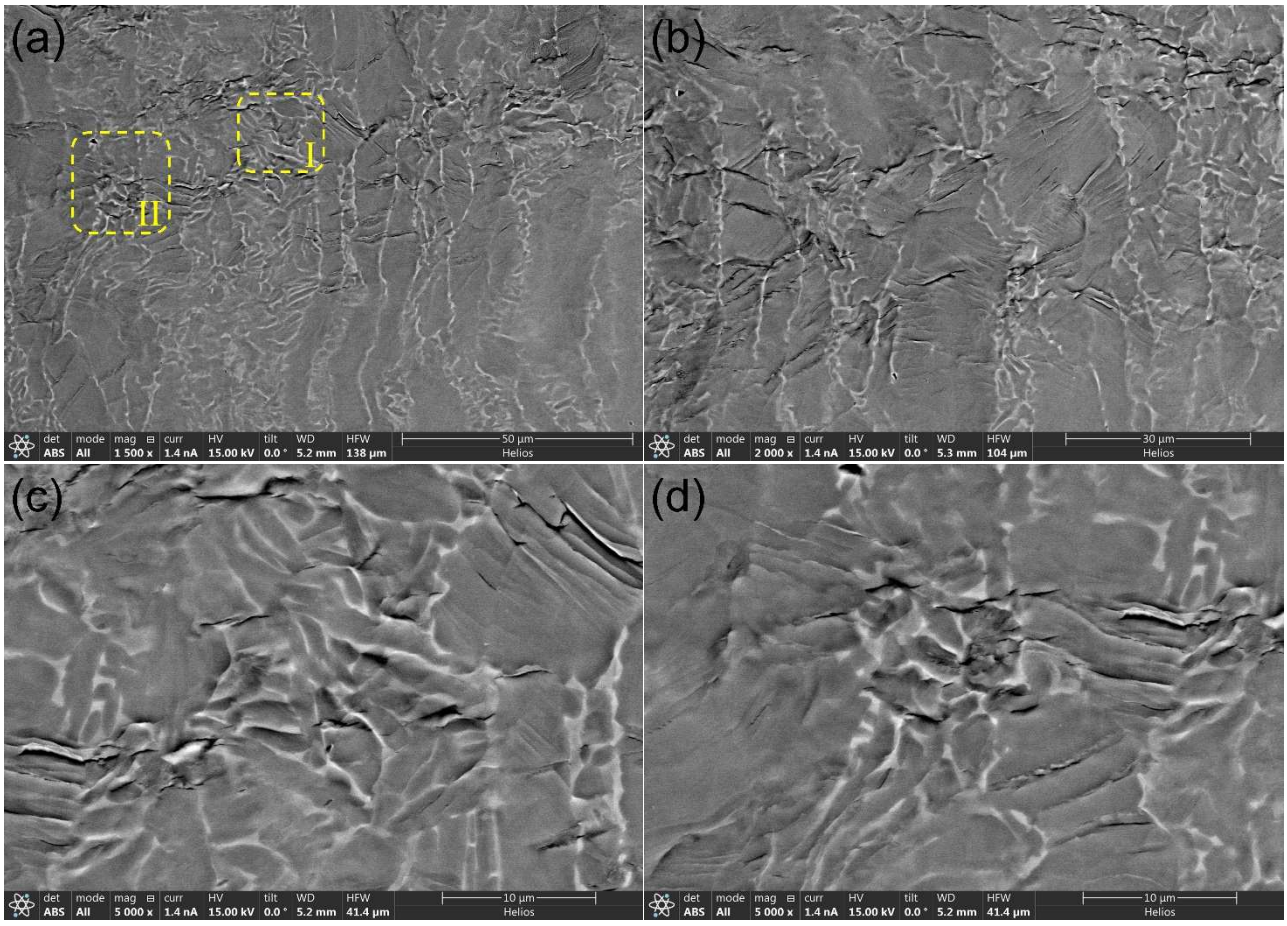

Fig. 3. (a) and (b) outer circumferential surface morphologies of a specimen failed due to interior crack initiation (σ_a = 580 MPa, N_f = 7.43×10^7 cycles), (c) and (d) microvoids nucleated in β_t (magnified image of Regions I and II in (a), respectively).

4. Conclusions

The VHCF properties and the damage mechanisms of a Ti-6Al-4V with needle-like β phase were investigated. The obtained fatigue lives vary from 3.56×10^5 cycles to 2.95×10^8 cycles for the applied stress levels ranging from 660 to 580 MPa. The interior crack-induced failure with a fish-eye pattern is the primary VHCF damage mode. The interior crack initiation results from the nucleation and coalescence of micro-voids and grooves in β_t, and the dominant microscopic mechanism causing VHCF fracture is the ductile crack nucleation instead of the commonly reported brittle one. The β_t phase plays a critical role in the crack initiation process, and strongly influences the fatigue properties of the Ti-6Al-4V alloy in the VHCF regime.

Acknowledgments

This work was funded by the National Natural Science Foundation of China (91860206) and Shaanxi Province Key Research and Development Program (2019KW-063).

References

[1] A. Shanyavskiy, Int. J. Fatigue 28(11) (2006) 1647-1657.

[2] F. Yoshinaka, T. Nakamura, S. Nakayama, D. Shiozawa, Y. Nakai, K. Uesugi, Int. J. Fatigue 93 (2016) 397-405.

[3] T. Gao, H. Xue, Z. Sun, D. Retraint, Mater. Sci. Eng., A 776 (2020) 138989.

[4] Y. Furuya, Materials Letters 112 (2013) 139-141.

[5] W. Li, H. Zhao, A. Nehila, Z. Zhang, T. Sakai, Int. J. Fatigue 104 (2017) 342-354.

[6] Y. Furuya, E. Takeuchi, Mater. Sci. Eng., A 598 (2014) 135-140.

[7] J. Everaerts, B. Verlinden, M. Wevers, Journal of Microscopy 267(1) (2017) 57-69.

[8] W. Li, M. Li, R. Sun, X. Xing, P. Wang, T. Sakai, Int. J. Fatigue 131 (2020).

[9] M.K. Dunstan, J.D. Paramore, Z.Z. Fang, J.P. Ligda, B.G. Butler, Int. J. Fatigue 131 (2020) 105355.

[10] X. Liu, C. Sun, Y. Hong, Int. J. Fatigue 92 (2016) 434-441.

[11] X. Liu, Y. Qian, Q. Fan, Y. Zhou, X. Zhu, D. Wang, 826 (2020) 154209.

[12] Z. Zhao, J. Chen, S. Guo, H. Tan, X. Lin, W. Huang, Journal of Materials Science and Technology 33(7) (2017) 675-681.

[13] S.K. Jha, C.J. Szczepanski, P.J. Golden, W.J. Porter, R. John, Int. J. Fatigue 42 (2012) 248-257.

[14] H. Shao, Y. Zhao, P. Ge, W. Zeng, Mater. Sci. Eng., A 559 (2013) 515-519.

[15] C. Lavogiez, S. Hémery, P. Villechaise, Scripta Materialia 183 (2020) 117-121.

[16] S. Joseph, I. Bantounas, T.C. Lindley, D. Dye, International Journal of Plasticity 100 (2018) 90-103.